

# Meta-reinforcement learning with minimum attention

**Shashank Gupta**

*Department of EECS  
University of Michigan  
Ann Arbor, MI 48109, USA*

SHASHANG@UMICH.EDU

**Pilhwa Lee**

*Department of Mathematics  
Morgan State University  
Baltimore, MD 21251, USA*

PILHWA.LEE@MORGAN.EDU

## Abstract

Minimum attention applies the least action principle in the changes of control concerning state and time, first proposed by Brockett. The involved regularization is highly relevant in emulating biological control, such as motor learning. We apply minimum attention in reinforcement learning (RL) as part of the rewards and investigate its connection to meta-learning and stabilization. Specifically, model-based meta-learning with minimum attention is explored in high-dimensional nonlinear dynamics. Ensemble-based model learning and gradient-based meta-policy learning are alternately performed. Empirically, the minimum attention does show outperforming competence in comparison to the state-of-the-art algorithms of model-free and model-based RL, i.e., fast adaptation in few shots and variance reduction from the perturbations of the model and environment. Furthermore, the minimum attention demonstrates an improvement in energy efficiency.

**Keywords:** Reinforcement learning, model-based RL, meta-learning, minimum attention

## 1 Introduction

Minimum attention considers the changes of control in state and time, first proposed by Brockett (Brockett, 1997), with the following criterion:

$$\mathcal{J}(u) = \frac{1}{2} \int_0^T \int_{\Omega} \left\| \frac{\partial u}{\partial x} \right\|^2 + \left\| \frac{\partial u}{\partial t} \right\|^2 dx dt, \quad (1)$$

highly relevant in emulating biological control, such as motor learning. As a first step for a rigorous analysis of minimum attention, the existence of the minimum attention was shown, focused on time-variant linear feedback control in the context of motor learning (Lee and Park, 2022). Interestingly, a similar framework was considered in the regularization of fluid flow control by Gunzburger. In the flow control of Navier-Stokes equations, the well-posedness of boundary flow control with the changes of control in time and space was proved by the one-shot method (Gunzburger and Manservisi, 2000). The minimum attention implies “regularization” and might work as stabilization in mathematical point of view, and provides a generative formalism of transition between “closed” and “open” loop controls (Lee and Park, 2022) from the control point of view.

In this paper, we apply minimum attention to the reward of reinforcement learning and investigate its connection to meta-learning. The primary motivation is that minimum at-

tention is a generative formalism of transition between feedforward and feedback controls while getting close to the target goals gradually in state and time (Lee and Park, 2022). This is conjectured to be associated with the adaptation to a new environment in the sense of meta-learning. Overall, the specific nature of the contributions is empirical in the following:

- Minimum attention has a significant improvement in total rewards.
- Minimum attention has a significant reduction in variance, implying the functionality of stabilization.
- Minimum attention has an enhancement of improved total reward in meta-testing.

This is indeed significant in its connection to safe RL and few shots of meta-learning. Most learning processes are through experiences, and their functionality is tested with new tasks. Deep reinforcement learning (RL) has been successful in showing competence in learning controls for complex systems (Mnih et al., 2015). Many of the algorithms are model-free and take the learning process purely by observing state transitions without explicit knowledge of internal system dynamics. As a consequence, most of those algorithms require a large number of sampling and immense learning time to come to a converging stage. Model-based RL shows a promising efficiency in sampling in comparison to model-free RL, but in many cases, the converging return is lower than the asymptotic performance of model-free RL due to model bias. Consequently, the main challenges are how to tolerate the inherent model-bias, and how the learned models and control are flexible to diverse tasks in the presence of uncertainties. Here, in our scope of consideration, two major uncertainties are attributed to 1) the model is not *a priori* known, and evolves in the model learning process, i.e., model-bias and 2) the model has intrinsic stochasticity or in the interaction with the environment. Model-ensemble approach with a number of models learned together shows a potential to overcome part of the issues (Clavera et al., 2018; Kurutach et al., 2018). In the paradigm of “learning to learn”, meta-learning pursues adaptation of learning with few shots confronting new tasks (Finn et al., 2017), showing a promising learning performance coupled to a model-ensemble approach (Clavera et al., 2018). In our strategy to handle the uncertainty of model learning, we also incorporate an ensemble of model systems in the course of model learning (Kurutach et al., 2018), utilizing data collected from the real environment.



Figure 1: Meta-learning from model and environmental perturbations. (a) Half-Cheetah with varying body masses (Lee et al., 2020), (b) Adaptation to uphill and downhill, (c) One hind leg crippled (Nagabandi et al., 2019)

Overall, related works on model-based RL and meta-RL, and the associated regularizations are covered in Section 2. We formulate the ensemble model-based meta-policy learning with

minimum attention in Section 3. In the main results of Section 4, the training/testing of high-dimensional dynamical systems is compared with the state-of-the art model-free and model-based RLs and analyzed in the feedback and feedforward terms and adaptation in model or environmental perturbations.

## 2 Related Works

**Model-based reinforcement learning** Once initially unknown or partially known models are reduced in model bias and uncertainty, and are well identified, model-based RL approaches can populate imaginary exploration and show outperforming learning curves with smaller samples for policy training. Taking a meta-learning with gradient-descent of a finite number model learning, i.e., ensemble model-based RL shows competent performances (Kurutach et al., 2018; Clavera et al., 2018). In the efforts of meta-learning and generalization, Lee et al. (2020) takes the dynamics model as a global one, which is learned by characterizing a context latent vector for the local dynamics and then by taking conditional prediction. Du et al. (2020) used neural-ODE in a model-based RL for semi-Markov decision processes in continuous-time dynamics.

**Reinforcement meta-learning** Model-agnostic meta-learning is by two-level gradient-based optimization in the sense of predictor-corrector schemes (Finn et al., 2017). For a rapid adaptation to a new environment, it is possible to take off-line learning (Clavera et al., 2018) or online learning (Nagabandi et al., 2019) at the test stage in model-based reinforcement learning. In the off-policy actor-critic methods, meta-critic is rapidly learned online for a single task, rather than slowly over a family of tasks (Zhou et al., 2020). In the technique of generalization, a loss function can be extended to encourage the context latent vector to be trained for predicting both forward and backward dynamics (Lee et al., 2020).

**Regularization in reinforcement learning and meta-learning** Regularization is important transforming non-convex profiles to convex and sparse discreteness to continuous and differentiable ones. In machine learning, robustness and domain generalization are fundamentally correlated, but "robustness" is neither necessary nor sufficient for transferability; rather, regularization is a more fundamental perspective for understanding domain transferability (Xu et al., 2022). In the inference of nonlinear state-space models, Corenflos et al. (2021) overcome the issue of traditional resampling encountering non-differentiable loss functions in partial filter methods with entropic regularization. Regularization with Jacobian term stabilizes the random and adversarial input perturbations in the classification without severely degrading generalization (Hoffman et al., 2019). Biased regularization overcomes complexities in distributions of tasks via a conditioning function which does mapping task's side information into a meta-parameter vector relevant for the specific task at hand (Denevi et al., 2020).

### 3 Ensemble model and meta-policy learning with minimum attention

#### 3.1 Mathematical formulation

Given the first-order nonlinear system,

$$\dot{x} = f(x, u, t), \quad (2)$$

where  $x \in \mathcal{X} \subseteq \mathbb{R}^n$  is the state,  $u \in \mathcal{U} \subseteq \mathbb{R}^m$  is the control, and  $f$  is continuously differentiable with respect to  $x$  and  $u$ . The corresponding stochastic differential equation is the following:

$$dx = f(x, u)dt + \sigma(x, t)dW_t. \quad (3)$$

#### 3.2 Model learning

The model  $\{\hat{f}_{\theta_M}\}$  parameterized by  $\theta_M$  is learned by the following loss function, similar to the approach of the probabilistic dynamics model (Clavera et al., 2018):

$$e(X_n, X_{n+1}) = \frac{X_{n+1} - X_n}{\Delta t_n} - \hat{f}_{\theta_M}(X_n, u(X_n)), \quad (4)$$

$$\mathcal{L}(\theta_M) = \frac{1}{|R|} \sum_{\{(X_n, X_{n+1})\} \in R} \|e(X_n, X_{n+1})\|^2, \quad (5)$$

where the data pool  $R$  with the transitions  $(X_n, X_{n+1})$  in the finite horizon is collected from the observation in the real environment.

#### 3.3 Meta-learning with model-ensemble

The control  $u = u_{\theta_u}(x)$  is defined by a feed-forward neural network with the parameter  $\theta_u$  and deterministically by the state  $x$ . The augmented hyperparameter  $\theta$  is the following:

$$\theta = \begin{bmatrix} \theta_u \\ \theta_M \end{bmatrix}. \quad (6)$$

The meta-learning by one-step gradient-ascent in policy optimization proceeds by two steps as follows:

$$r_{\text{reg}}(x, u_{\theta}) = r(x, u_{\theta}) - \alpha(\|\frac{\partial u_{\theta}}{\partial x}\|^2 + \|\frac{\partial u_{\theta}}{\partial t}\|^2), \quad (7)$$

$$\mathcal{J}_i(\theta) = \mathbb{E}_{\mathcal{T}_i} \left( \int_0^T r_{\text{reg}}(x, u_{\theta}) dt \right), \quad (8)$$

where the sample trajectories  $\mathcal{T}_i$  are generated by model  $\mathcal{M}_i$  and the control  $u_{\theta}$ . Based on the vanilla policy gradient method (Peters and Schaal, 2006):

$$\nabla_{\theta_u} \mathcal{J}_i(\theta) = -\mathbb{E}_{\mathcal{T}_i} \left( \sum_{k=0}^T \nabla_{\theta_u} \log P_i(x_k, t_k; \theta) \left( \sum_{l=k}^T \gamma^l r_{\text{reg}}(x_l, u_{\theta}(x_l)) - b_k \right) \right), \quad (9)$$

$$\theta'_{u,i} = \theta_u + \beta \nabla_{\theta_u} \mathcal{J}_i(\theta), \quad (10)$$

which is the first one-step gradient-ascent for adaptation of policy. Next is integrating the return utilizing the whole model-ensemble  $\{\mathcal{M}_i\}$ :

$$\begin{aligned}
r_{\text{reg}}(x, u_{\theta'_i}(x)) &= r(x, u_{\theta'_i}(x)) - \alpha(\|\frac{\partial u_{\theta'_i}}{\partial x}\|^2 + \|\frac{\partial u_{\theta'_i}}{\partial t}\|^2), \\
\max_{\theta_u} \quad & \frac{1}{M} \sum_i^M \mathcal{J}_i(\theta') \quad \text{s.t.} \\
\mathcal{J}_i(\theta') &= \mathbb{E}_{\mathcal{T}'_i} \left( \int_0^T r_{\text{reg}}(x, u_{\theta'_i}(x)) dt \right),
\end{aligned} \tag{11}$$

where the sample trajectories  $\mathcal{T}'_i$  are generated by the model  $\mathcal{M}_i$  and the adapted control  $u_{\theta'_i}$ .

### 3.4 Trust Region Policy Optimization (TRPO)

Based on the trust region policy optimization (TRPO) (Schulman et al., 2015),

$$\begin{aligned}
\max_{\theta} [\nabla_{\theta} \mathcal{J}(\theta_u) \cdot (\theta'_u - \theta_u)] \\
\text{subject to } \frac{1}{2} \|\theta'_u - \theta_u\|^2 \leq \delta
\end{aligned} \tag{12}$$

where  $\nabla_{\theta_u} \mathcal{J}_{\theta}$  follows Vanilla Gradient Policy (VPG) in Equation (9).

### 3.5 Formulation of control: linearization with stochastic terms

The control  $\mathbf{u}$  is linearized in state of  $\mathbf{x}$  with feedback gain of  $\mathbf{K}(\mathbf{t})$  and feedforward term of  $\mathbf{v}(\mathbf{t})$ :

$$\mathbf{u}(\mathbf{x}, t) = \mathbf{K}(\mathbf{t})\mathbf{x} + \mathbf{v}(\mathbf{t}) + \epsilon, \tag{13}$$

where the stochastic term of control,  $\epsilon$  is formulated by Gaussian noise or Ornstein-Uhlenbeck process (Uhlenbeck and Ornstein, 1930):

$$d\epsilon = \theta_{\text{OU}}(\mu - \epsilon)dt + \sigma_{\epsilon}dW_{\epsilon}. \tag{14}$$

where  $\theta_{\text{OU}}$  and  $\sigma_{\epsilon}$  are the involving relaxation and stochasticity constants.

## 4 Main Results and Discussion

We explore the performance of the proposed ensemble model-based meta-learning with minimum attention to show the following:

- Is the proposed algorithm competent in the required training sampling in comparison to other model-based RL?
- Does the proposed algorithm reduce the variance in learning curves?
- Does the proposed algorithm improve generalization in comparison to other model-based meta-policy RL?

**Algorithm 1** Meta-learning with minimum attention

---

```

Initialize  $\theta_i = [\theta_{\mathcal{M}}^i \theta_u]$ ;  $\theta_{\mathcal{M}}^i$  for model  $\mathcal{M}_i$  and  $\theta_u$  for the control.
The model ensemble  $\mathcal{M} = \{\mathcal{M}_i\} = \{\hat{f}_i\}_{i=1}^M$ 
 $R_i \leftarrow \emptyset$ 
for  $epoch = 1$  to  $T_{\text{epoch}}$  do
  {Model learning}
  for  $i = 1$  to  $M$  do
    Sample trajectories  $\{X_n^i\}$  from the environment with  $[\theta_{\mathcal{M}}^i \theta'_{u,i}]$ , and  $R_i \leftarrow \{X_n^i\}$ :
    Train  $\mathcal{M}_i$  using  $R_i$  and  $\mathcal{L}(\theta_{\mathcal{M}})$  in Eq. (5).
  end for
  {Meta-policy learning}
  for  $i = 1$  to  $M$  do
    Generate  $\{x_j^k\}$  with  $x_j^0 \sim \rho_i(\cdot, 0)$  and the sample size  $N$ .
    This is to sample model-based "imaginary" trajectories  $\mathcal{T}_i$  from  $\mathcal{M}_i$  using  $\theta_i$ .
     $\mathcal{J}_i(\theta) \leftarrow \frac{1}{N} \sum_{k,j} r(x_j^k, u_{\theta}(x_j^k, t_k))$ 
     $\mathcal{J}_i(\theta) \leftarrow -\frac{\alpha}{N} \sum_{k,j} (\|\frac{\partial u_{\theta}}{\partial x}\|^2 + \|\frac{\partial u_{\theta}}{\partial t}\|^2)(x_j^k, t_k)$ 
    Adapt parameters  $\theta'_{u,i} = \theta_u + \beta \nabla_{\theta_u} \mathcal{J}_i(\theta)$  with VPG/SAC.
    Sample model-based trajectories  $\mathcal{T}'_i$  from  $\mathcal{M}_i$  using adapted  $u_{\theta'_i}$ :
    Generate  $\{x_j^k\}$  with  $x_j^0 \sim \rho'_i(\cdot, 0)$  and the sample size  $N$ .
     $\mathcal{J}_i(\theta') \leftarrow \frac{1}{N} \sum_{k,j} r(x_j^k, u_{\theta'_i}(x_j^k, t_k))$ 
     $\mathcal{J}_i(\theta') \leftarrow -\frac{\alpha}{N} \sum_{k,j} (\|\frac{\partial u_{\theta'}}{\partial x}\|^2 + \|\frac{\partial u_{\theta'}}{\partial t}\|^2)(x_j^k, t_k)$ 
  end for
  Train  $\theta_u$  using  $\frac{1}{M} \sum_i \mathcal{J}_i(\theta')$  in Eq. (11) with TRPO.
end for

```

---

We conduct a series of experiments across several MuJoCo environments to rationalize the proposed method. The evaluation is designed to demonstrate that the minimum attention regularization: 1) improves asymptotic performance and learning stability; 2) induces policies that are smoother and more energy-efficient by learning a more structured control strategy; and 3) enhances an agent's ability to rapidly adapt to out-of-distribution (OOD) perturbations.

We present results for HalfCheetah in detail, followed by summaries for Hopper, Walker2d, and Humanoid to demonstrate the generality of our findings.

#### 4.1 Experimental setup: high-dimensional dynamical systems

Our method integrates the minimum attention regularization into the actor-critic updates of a state-of-the-art model-based meta-learning framework, MB-MPO (Clavera et al., 2018), which uses SAC (Haarnoja et al., 2018) for policy optimization. We compare against the original MB-MPO and a purely model-free SAC as baselines.

We mainly explore motor learning and control of four agents of MuJoCo in the OpenAI Gym (Brockman et al., 2016): Half-Cheetah (17-dim states and 6-dim controls), Walker2D (17-dim states and 6-dim control), Hopper (11-dim states and 3-dim controls), and HumanoidTruncated (45-dim states and 17-dim controls). The governing equations for MuJoCo

dynamics are formulated by Eqs. (3, 13, 14). The involved learning processes are alternated between model learning and meta-policy learning, and with or without regularization of minimum attention laws. In regard to hyperparameters, key hyperparameters for the Model-Based Meta-Policy Optimization (MB-MPO) with minimum attention implementation and the baseline are described in Appendix A. In general evaluation, we have used 10 random seeds for training episodes. For the final evaluation of a trained agent, we run 10 episodes per seed, i.e., with the randomized initial configuration. Unless otherwise specified, results are averaged over 10 random seeds, with error bands and  $\pm$  values indicating one standard deviation. A comprehensive description of all network architectures and hyperparameters is provided in Appendix A. Average total reward, standard deviation/error of reward across seeds/episodes are shown in Figure 2 and 3.

In the meta-training, to analyze the effect of attention weight, we trained agents with attention weight values  $\alpha \in \{0, 0.01, 0.05, 1.0, 5.0\}$  while keeping all other hyperparameters same. In order to analyze the effects of the number of ensemble models,  $M$ , we trained 4 different sizes of  $M \in \{1, 5, 15, 20\}$ . To characterize the effect of the imaginary trajectory size  $N$  in the MB-MPO inner loop, we trained the motor learning with 4 different values of  $N \in \{16, 128, 256, 512\}$  (Figure 4).

In regards to specific metrics, 1) average feedback norm: during evaluation, we run the trained agent for 10 evaluation episodes and average  $\|\partial u / \partial x\|^2$  per step, 2) average feedforward norm: define as the averaged  $\|\partial u / \partial t\|^2$  over 10 evaluation episodes, 3) average energy: define total sum  $\|u^2\|$  per step as “control cost”. Their time courses are shown in Figure 5. Heatmaps of the Jacobian norm (Figure 6, Figure S1, S4, S7) and jerk norm (Figure 7, Figure S2, S5, S8) between the baselines are shown to qualitatively judge the impact of minimum attention regularization.

In the meta-testing, experiments focus on out-of-distribution tasks and fast adaptation during meta-loop test time evaluation. For each of these experiments, we note the total reward, standard deviation between runs, average feedback, average feedforward norm, and average used energy. With the meta-trained agent, we have evaluated the impact of minimum attention regularization on the learning process by conducting qualitative analysis by visualizing policy sensitivity across different observation of the state with a specific dimension of the environment. The goal is to pick the dimensions that are critical for their respective locomotion and balance challenges. Specifically, we have picked Half-Cheetah, and three projections are plotted by heatmap: Torso height versus forward velocity, Forward velocity versus vertical velocity, and Forward velocity versus angular velocity. Similarly, the projected dimensions for other agents are specified in Appendix A.

## 4.2 The details of the algorithm implementation

In regard to core Model-Based Policy Optimization (MB-MPO) components, for inner and outer loop policy updates, we have experimented with Proximal Policy Optimization (PPO) (Schulman et al., 2017), Trust Region Policy Optimization (TRPO), and Soft Actor-Critic (SAC) (Haarnoja et al., 2018). We have experimented with 4 different imagi-

	Half-Cheetah	Hopper	Walker2D	Humanoid
MB-MPO training	$6692 \pm 318$	$2475 \pm 3.81$	$2399 \pm 694$	<b><math>575 \pm 177</math></b>
MB-MPO meta-testing	$6356 \pm 132$	$467 \pm 100$	$523 \pm 174$	$315 \pm 67$
MB-MPO + Min Attn training	<b><math>9721 \pm 128</math></b>	<b><math>2825 \pm 1.25</math></b>	<b><math>3038 \pm 148</math></b>	$352 \pm 38$
MB-MPO + Min Attn meta-testing	<b><math>6822 \pm 109</math></b>	<b><math>485 \pm 61</math></b>	<b><math>1123 \pm 152</math></b>	<b><math>480 \pm 34</math></b>

Table 1: Comparison of the model-based RL (MB-MPO) with regularization of minimum attention in meta-training and testing. Total reward at the epoch of 200K. For Hopper, the thigh is paralyzed. For Walker2D, the right thigh is paralyzed.

nary trajectory sample sizes  $N$ : 16, 128, 256, and 512. Specifically, the regularization term  $\|\partial u_\theta / \partial x\|^2 + \|\partial u_\theta / \partial t\|^2$ , is added to the policy loss with weight “ $\alpha$ ”. We have experimented for “ $\alpha$ ” taking values 0.01, 0.05, 1.0, and 5.0.

The “meta-learning” loop essentially follows that of Model-Agnostic Meta-Learning (MAML) structure (inner loop for the perturbation of models, outer loop for the optimization of meta-parameters): tasks (models) are sampled randomly from the task list, the mini-batch of  $R_i$  in Algorithm 1. Specifications of the inner loop, and outer loop are in parameters (Appendix A). For model ensemble setup, we have experimented with four different models of ensemble size: 1, 5, 15, and 20. Some details of the neural network architecture are provided in the Appendix A (Dynamics model ensemble).

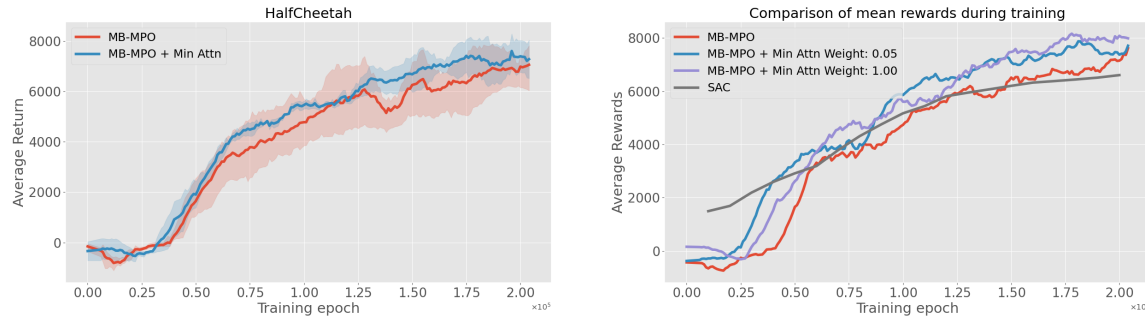


Figure 2: (a) Training of Half-Cheetah. There is a reduction of variance from minimum attention, (b) Comparison of learning curves among model-free RL (SAC, (Haarnoja et al., 2018)) and model-based RL (MB-MPO, (Clavera et al., 2018), the proposed MB-MPO + minimum attention, weighting factor  $\alpha = 0.05$  and 1). The experiment is run with 10 episodes.

#### 4.3 Dependency on the ensemble model size and imaginary sample size

Figure 4 shows the influence of the ensemble model size of  $M$  and the imaginary sample size of  $N$ . When the ensemble model size of  $M$  increases to 20, the total reward also increases.

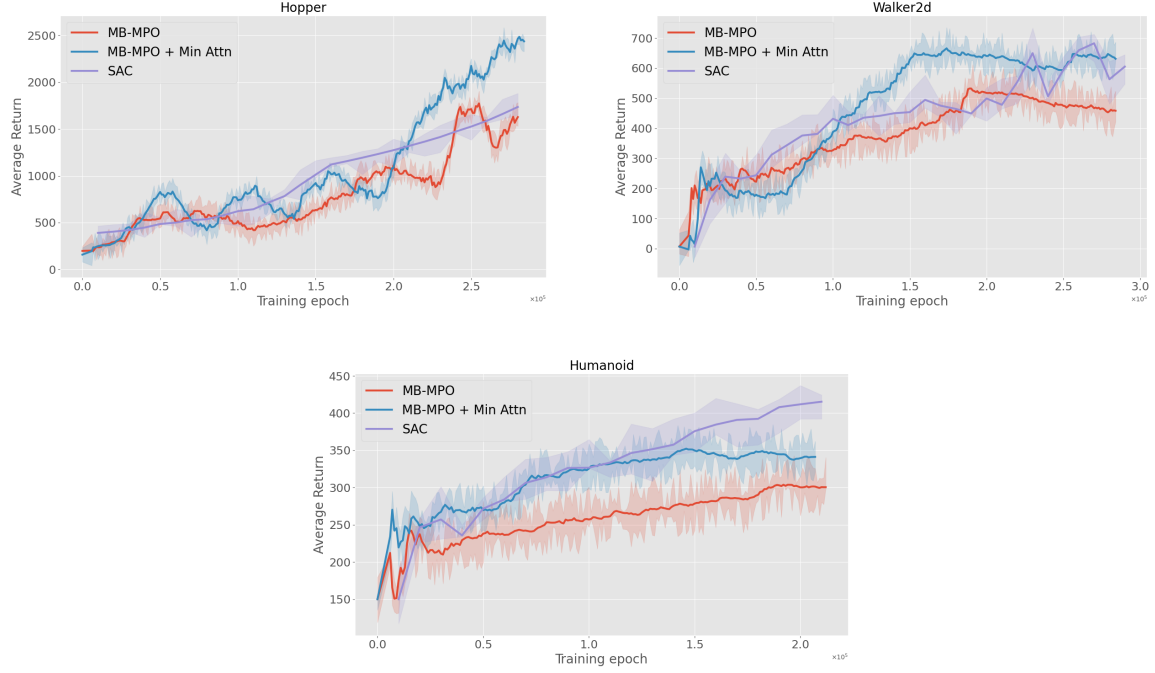


Figure 3: Meta-Training with different models, (a) Hopper, (b) Walker2D, (c) Humanoid. The model-based RL (MB-MPO) is employed with and without minimum attention ( $\alpha = 1.0$ ) and compared with SAC.

The imaginary sample size  $N$  provides the benefit of increased total reward to  $N = 128$ , but decreases when  $N$  is increased to 256.

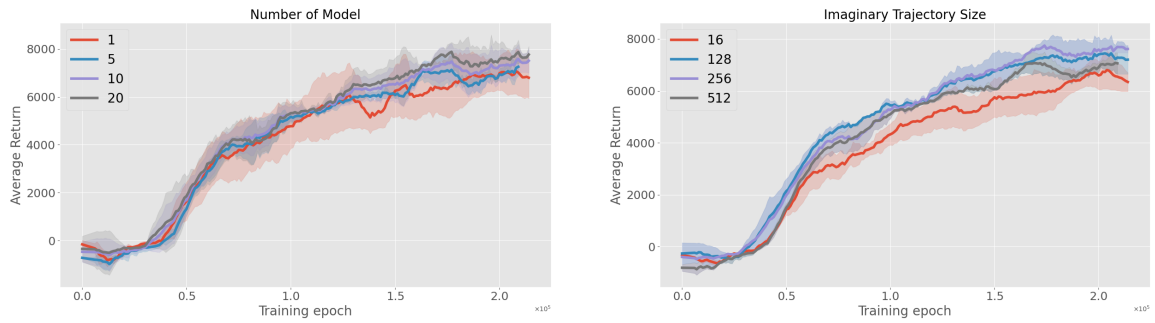


Figure 4: Half-Cheetah: Dependency on the ensemble model size and imaginary rollouts. When the ensemble model size of  $M$  increases to 20, the total reward also increases. The imaginary sample size  $N$  provides the benefit of increased total reward to  $N = 128$ , but decreases when  $N$  is turned to 256.

	MB-MPO	Ours ( $\alpha = 1.0$ )	Ours ( $\alpha = 0.01$ )	Ours ( $\alpha = 0.05$ )
<b>Meta-training</b>				
Average total rewards	$6692 \pm 318$	<b><math>9721 \pm 128</math></b>	$7545 \pm 123$	$8385 \pm 179$
Average feedback normalized	$783 \pm 135$	<b><math>567 \pm 53</math></b>	$590 \pm 88$	$637 \pm 56$
Average feedforward normalized	$5.16 \pm 0.11$	<b><math>5.01 \pm 0.07</math></b>	$5.02 \pm 0.10$	$5.05 \pm 0.07$
Average energy normalized	$4.54 \pm 0.13$	<b><math>3.85 \pm 0.05</math></b>	$3.94 \pm 0.03$	$3.91 \pm 0.02$
<b>Meta-testing</b>				
Average total rewards	$6356 \pm 132$	<b><math>6822 \pm 109</math></b>	$6514 \pm 133$	$6590 \pm 125$
Average feedback normalized	$673 \pm 75.6$	<b><math>625 \pm 34.7</math></b>	$650 \pm 77.4$	$720 \pm 53.9$
Average feedforward normalized	$7.03 \pm 0.04$	<b><math>6.76 \pm 0.04</math></b>	$4.87 \pm 0.04$	$7.07 \pm 0.04$
Average energy normalized	$372 \pm 2.71$	<b><math>366 \pm 1.48</math></b>	$334 \pm 1.12$	$359 \pm 1.58$

Table 2: Half-Cheetah: **Meta-training**: total reward, feedback ( $\|\partial u / \partial x\|^2$ , Jacobian), feedforward ( $\|\partial u / \partial t\|^2$ , jerk), and energy ( $\|u\|^2$ ) at final stage of iterations (200K). Comparison of the model-based RL (MB-MPO) without and with regularization of minimum attention. The bold typeset represents the best outperformance in the variation of  $\alpha$ . **Meta-testing**: the agent of Half-Cheetah, one leg crippled, at final stage of iterations (200K).

#### 4.4 Comparison with state-of-the-art RL algorithms

The comparison is mostly based on the performance on standard locomotion tasks. We consider a model-free RL, SAC (Soft Actor-Critic) (Haarnoja et al., 2018) and a model-based RL, MB-MPO (Model-Based Meta-Policy Optimization) (Clavera et al., 2018). Firstly, we show the training of Half-Cheetah (Figure 2) in comparison of learning curves among the model-free RL (SAC), the model-based RL (MB-MPO), and the proposed MB-MPO with minimum attention, where the weighting factor is  $\alpha = 0.01, 0.05$ , and  $1$ . We have experienced a statistically significant reduction of variance from minimum attention. To demonstrate the generality of our approach, Figure 3 presents the learning curves for Hopper, Walker2D, and Humanoid. Across all three kinematically distinct agents, our method (MB-MPO + minimum attention, blue) consistently converges to a higher average return than the vanilla MB-MPO baseline (red). *For the complex Humanoid task, our method also exhibits noticeably lower variance, indicating a more stable and reliable learning process.*

The outperformance of MB-MPO with minimum attention is quantified in numbers in Table 1 and 2. Table 2 provides a detailed quantitative summary of the final performance on HalfCheetah after 200K iterations. In the standard meta-training setting, the best minimum attention factor ( $\alpha = 1.0$ ) achieves a 45% higher reward than MB-MPO, while simultaneously reducing the average feedback norm (Jacobian) by 28% and energy consumption by 15%. This demonstrates that the regularization does not trade performance for smoothness, but rather enables the discovery of policies that are both higher-performing and more efficient. Crucially, in the meta-testing scenario where the agent must adapt to a crippled leg, the performance benefits of our method are maintained or even amplified. The half-cheetah with minimum attention achieves a higher reward ( $6822 \pm 109$ ) than the vanilla baseline ( $6356 \pm 132$ ) and does so with a lower feedback norm and feedforward norm (jerk). *This suggests that the smoother policies learned through minimum attention provide a better prior for rapid adaptation to significant out-of-distribution embodiment changes.*

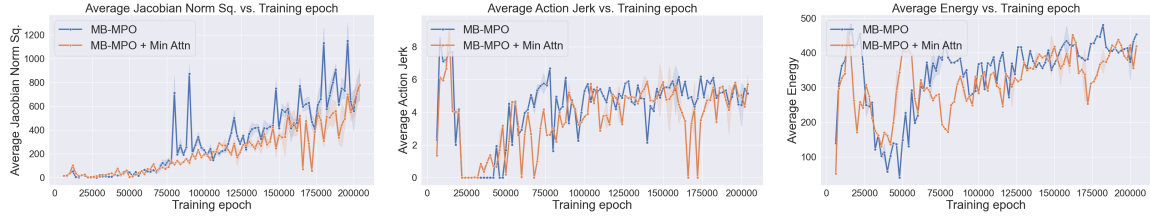


Figure 5: Half-Cheetah: Time profiles for the feedback, feedforward, and energy in training. The comparison of feedback ( $\|\partial u/\partial x\|^2$ , Jacobian), feedforward ( $\|\partial u/\partial t\|^2$ , Jerk), and energy ( $\|u\|^2$ ) between MB-MPO and MB-MPO with minimum attention ( $\alpha = 1.0$ ).

We first establish the performance of our method on standard locomotion tasks. Figure 2 presents the learning curves on HalfCheetah, comparing our method against model-based (MB-MPO) and model-free (SAC) baselines. Our approach not only matches the sample efficiency of MB-MPO but also converges to a significantly higher average reward. Notably, the learning curves of our method also exhibit reduced variance across episodes, suggesting a more stable and reliable learning process, a key benefit for safe RL. This trend of superior performance and stability generalizes across other agents, as shown by the learning curves for Hopper, Walker2D, and Humanoid in Figure 3. Quantitative summary for all tested environments can be found in Appendix B.

Time profiles for the feedback, feedforward, and energy in training are shown in Figure 5. Furthermore, we analyze the evolution of these policy characteristics throughout the training process. The benefits of our regularization are present from the early stages of learning. The average feedback norm for our method remains consistently below the baseline after an initial exploration phase, and energy consumption is also markedly reduced. This confirms that minimum attention actively shapes the policy towards smoother and more efficient solutions during the entire learning process.

#### 4.5 Analysis of learned control strategies of minimum attention

To understand how minimum attention achieves superior performance, we conduct a qualitative analysis of the learned control strategies. We interpret the minimum attention's two components as proxies for distinct control paradigms: the spatial term,  $\|\partial u/\partial x\|^2$  (feedback norm or Jacobian), measures the policy's reactive sensitivity to state changes, while the temporal term,  $\|\partial u/\partial t\|^2$  (feedforward norm or jerk), measures the smoothness of the action sequence over time.

#### SHIFTING THE CONTROL LANDSCAPE IN HALF-CHEETAH

First, we visualize the underlying control landscape using heatmaps for the HalfCheetah agent. Figure 6 compares the spatial sensitivity (feedback norm or Jacobian) of the vanilla MB-MPO policy against our regularized method. A clear narrative emerges across the different state-space projections:

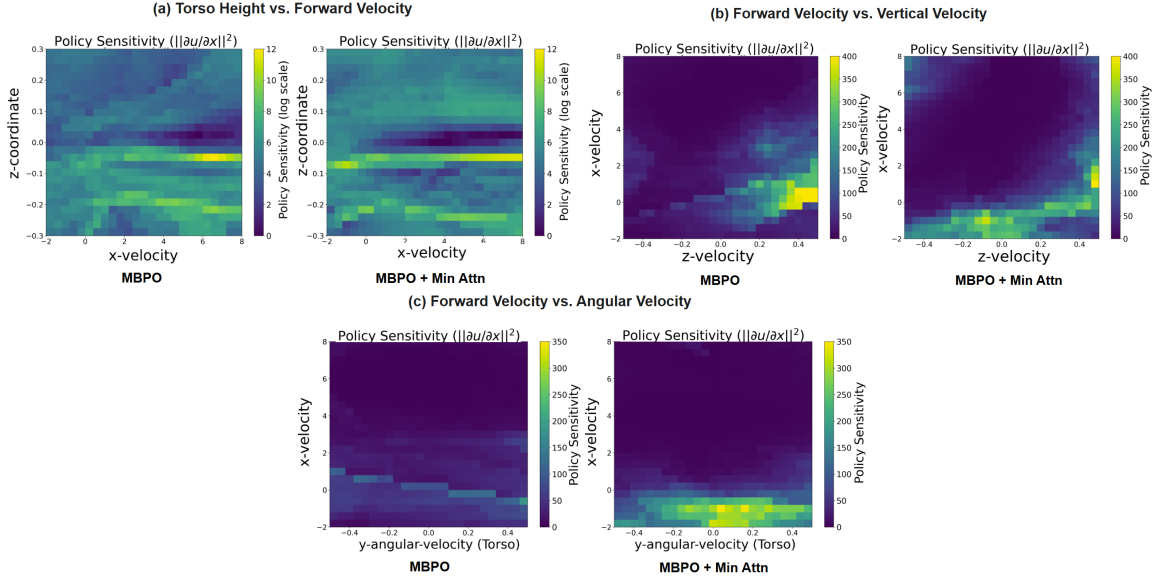


Figure 6: Heatmap of feedback. With Half-Cheetah, the feedback ( $||\partial u / \partial x||^2$ ) in the projection of the states to a) X velocity and Z coordinates, b) Z velocity and X velocity, and c) Y angular velocity and X velocity. In the projections to X velocity and Z coordinates as well as Y angular velocity and X velocity, the minimum attention slightly regularizes the localized peak. In the projection to Z velocity and X velocity, the minimum attention makes the feedback reinforced and spread out. Heatmaps of policy sensitivity ( $||\partial u / \partial x||^2$ , log scale for (a)) for HalfCheetah, comparing vanilla MB-MPO and our method with minimum attention. **(a)** Torso height vs. forward velocity: Our method learns a simpler strategy with a stable base posture, reducing sensitivity at high speeds. **(b)** Forward velocity vs. vertical velocity: Our method distributes sensitivity over a wider range of vertical velocities, avoiding sharp reactive hotspots. **(c)** Forward velocity vs. angular velocity: Our method induces a proactive stabilization mechanism, showing higher sensitivity to torso roll at low speeds.

- **In locomotion (Figure 6a, height vs. velocity):** The vanilla policy learns a complex, reactive strategy with high sensitivity at high speeds. Our regularization encourages a simpler, more robust base posture, drastically reducing sensitivity and demonstrating a more efficient control strategy.
- **In vertical motion (Figure 6b, velocity vs. Z-velocity):** The vanilla policy relies on a concentrated, high-magnitude "hotspot" of sensitivity to manage the take-off phase. Our method distributes this control effort over a wider range of vertical velocities, replacing the sharp, reactive correction with a smoother, more continuous control function.
- **In stabilization (Figure 6c, velocity vs. angular velocity):** A key strategic difference is revealed. While the vanilla policy is largely passive to torso roll at low speeds, our regularized policy learns a proactive stabilization mechanism, actively applying corrections in this vulnerable regime to prevent future instability.

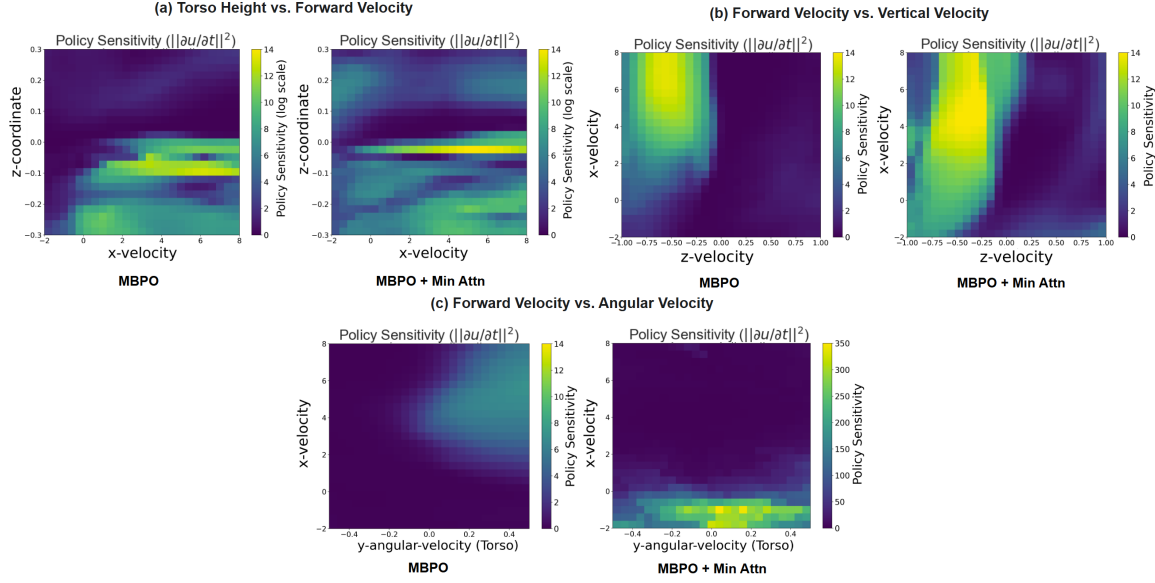


Figure 7: Heatmaps of policy jerk ( $||\partial u / \partial t||^2$ ) for HalfCheetah. Our method concentrates propulsive jerk and introduces a novel, proactive stabilization behaviour against torso roll at low speeds.

Figure 7 shows a similar analysis for temporal sensitivity (jerk). The regularized policy is seen to concentrate its propulsive jerk into more precise phases of the gait cycle, while again introducing proactive, stabilizing jerk to counter torso roll at low speeds—a behavior absent in the baseline. Taken together, these visualizations show a clear shift from a reactive, sporadic control strategy to a proactive, structured, and efficient one. Similarly, more detailed analysis is provided for Hopper, Walker2D, and Humanoid in Appendix B.

Effect of minimum attention regularization (Figure 6) is analyzed in two folds.

#### REDUCED PEAK SENSITIVITY

The most striking difference is the lower maximum sensitivity in the attention-based policy. This is exactly what one is to see if the “minimum attention” (feedback and feedforward, Jacobian and jerk norms) regularization is working. It penalizes large derivatives, effectively “smoothing” the policy and preventing excessively sharp changes in action for small state changes.

#### DISTRIBUTION OF SENSITIVITY

The attention-based policy might be “spreading out” its necessary sensitivity or making it more localized. The vanilla policy seems to have a more concentrated “hotspot” of extremely high sensitivity. The attention mechanism might be encouraging the policy to be smoother in general, only allowing higher sensitivity where it is deemed more critical by the trade-off between task performance and the regularization penalty.

Specifically, there are task-relevant regions so that both policies identify a similar region (low Z-coord, high forward velocity) as requiring high sensitivity. This region in Half-

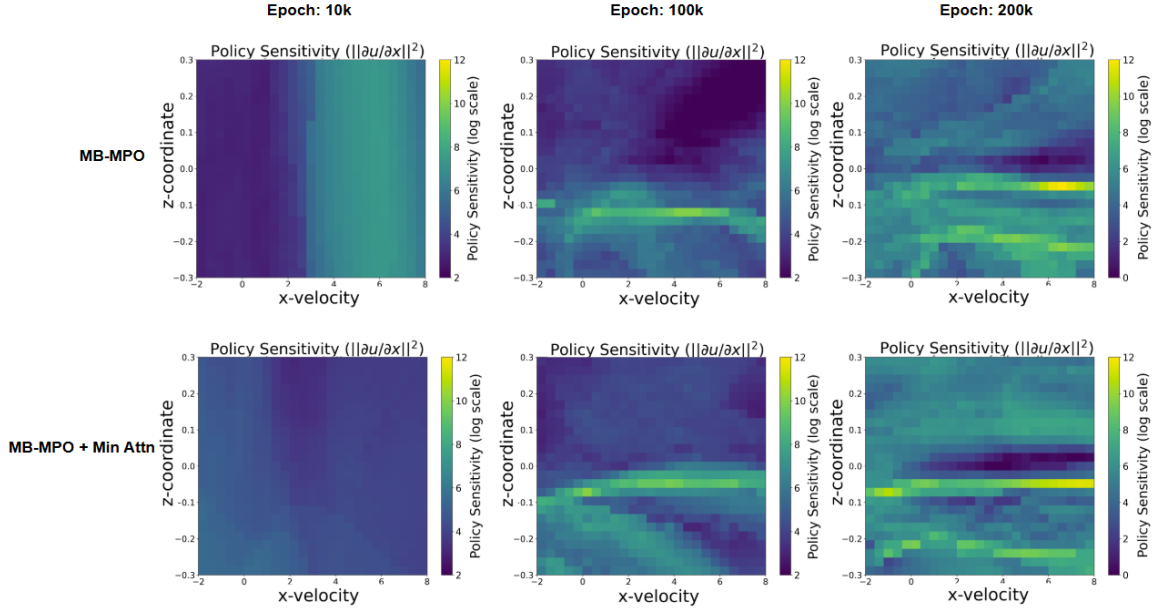


Figure 8: Evolution of spatial sensitivity (feedback norm,  $\|\partial u / \partial x\|^2$ ) for HalfCheetah. **Top Row (MB-MPO):** Converges to a broadly reactive strategy. **Bottom Row (Ours):** Converges to a sparse, structured strategy, focusing sensitivity on a critical phase.

Cheetah could correspond to maintaining balance at high speed: Small changes in torso pitch (related to Z-coord) or velocity might require significant control adjustments to prevent falling. Nearing a terminal state or a critical phase of locomotion: The policy might need to be very responsive here. The fact that both policies highlight similar locations for high sensitivity suggests these are indeed critical areas dictated by the environmental dynamics and task. The magnitude of sensitivity in these critical areas is what the regularization seems to affect.

In regards to policy “strategy”, the vanilla policy might be learning a more “aggressive” or “reactive” strategy in certain critical regions, leading to very strong feedback (high Jacobian norms). This could be optimal for pure reward maximization but potentially less robust or energy-efficient. Attention-based policy learns to achieve the task while keeping control effort (sensitivity) lower. It still becomes sensitive where needed, but perhaps not to the same extreme degree. This could lead to smoother transitions and less jerky movements, better energy efficiency (if actions are related to energy), and potentially increased robustness to small perturbations if extreme sensitivity is not required.

In terms of areas of low sensitivity, in regions where both plots are dark purple, the policies are relatively insensitive to small state changes. These might be “stable” regions of the state space where the current action strategy is robust, or where the agent is far from critical transitions.

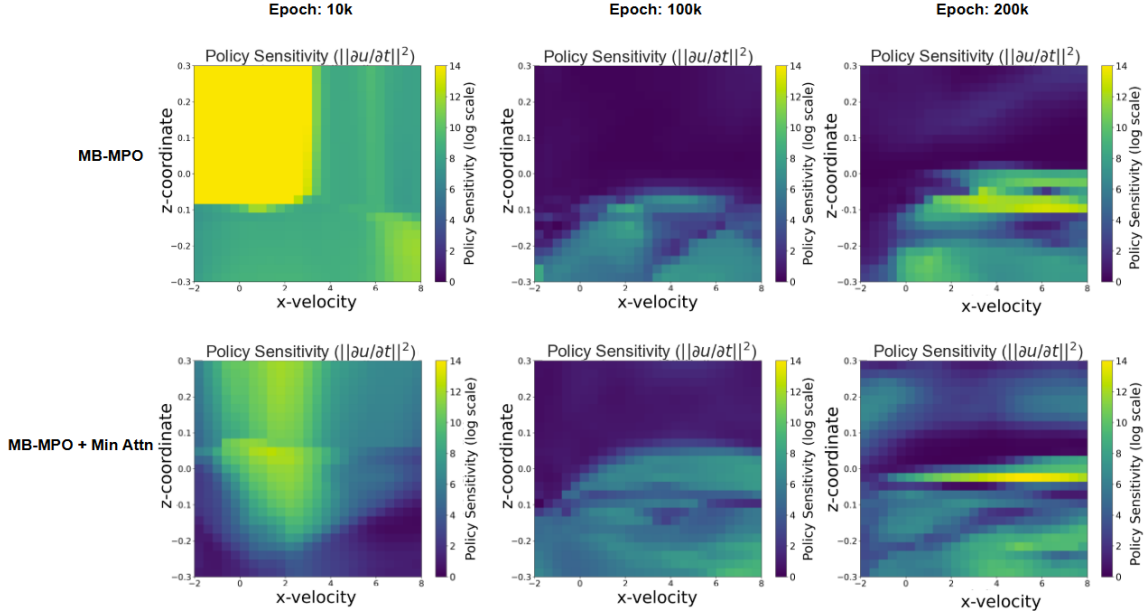


Figure 9: Evolution of temporal sensitivity (feedforward norm/jerk,  $||\partial u / \partial t||^2$ ) for HalfCheetah. **Top Row (MB-MPO):** Progresses from chaotic flailing to a moderately jerky running gait. **Bottom Row (Ours):** The regularizer shapes the policy to be smoother overall, concentrating its action changes into a single, precise phase of the gait cycle.

#### MATURATION OF LEARNED CONTROL STRATEGIES

To understand how the final control strategies emerge, we visualize the evolution of both spatial sensitivity (feedback/Jacobian norm) and temporal sensitivity (feedforward/jerk) at different stages of training. Figures 8 and 9 show the policy heatmaps for HalfCheetah at 10K, 100K, and 200K epochs for both vanilla MB-MPO and our regularized method.

**Maturation of feedback (Jacobian) strategy (Figure 8):** At the early stage of training (10K epochs), both policies exhibit broad, unstructured sensitivity. As training progresses, a clear divergence in strategy appears. The vanilla MB-MPO policy (top row) develops a wide, high-sensitivity band at high forward velocities, indicating it has learned a reactive strategy that requires constant, high-gain corrections to maintain a running gait. In contrast, our regularized policy (bottom row) converges to a much sparser and more structured landscape. It learns to be largely insensitive across most of the state space, focusing its sensitivity into a narrow, precise band corresponding to the apex of its running motion. This shows the minimum attention actively guides the policy towards a simpler, more efficient state-action mapping.

**Maturation of feedforward (jerk) strategy (Figure 9):** The evolution of temporal sensitivity is even more striking. The vanilla MB-MPO policy (top row) begins with ex-

tremely high, undifferentiated jerk at low speeds (10K epochs), essentially an exploratory behavior. As it learns, it suppresses this initial jerk but retains a moderately high level of action change during the low-crouch running phase (200K epochs).

The minimum attention policy (bottom row) follows a different developmental path. While it also explores with high jerk initially, the minimum attention quickly shapes the policy to be temporally smoother overall. By the final stage (200K epochs), it has learned a highly specialized strategy: the jerk is concentrated into a very sharp, narrow band at a specific torso height. This suggests the agent has learned an efficient, ballistic motion, where it "coasts" with smooth actions for most of the gait cycle and applies a single, decisive, and well-timed control change at the critical take-off point.

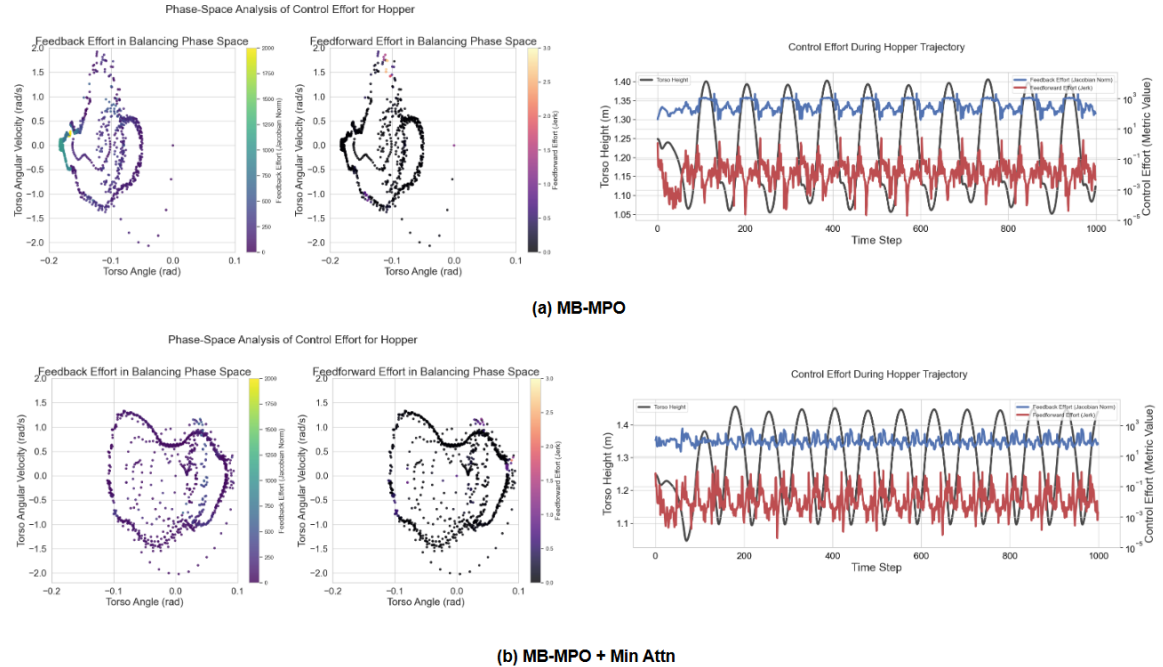


Figure 10: Left Column: Phase-space analysis of control effort for Hopper’s balancing motion. **Top Row (MB-MPO):** A “panic” strategy with an extreme feedback hotspot ( $> 2000$ ) for backward leans. **Bottom Row (Ours):** A smooth, proactive strategy with distributed, low-gain feedback, eliminating the need for high-gain emergency corrections. Right Column: Control effort during a Hopper trajectory. **Top (MB-MPO):** Shows massive, periodic feedback spikes at the bottom of each hop. **Bottom (Ours):** Exhibits a more regular gait with dramatically lower and smoother control effort.

#### DYNAMIC CONSEQUENCES IN HOPPER

These fundamental changes in the control landscape lead to qualitatively different and more stable behaviors. We illustrate this using phase-space and time-series analyses of the Hopper agent in Figure 10. This figure provides both a phase-space portrait of the balancing

strategy and a time-series view of the control effort throughout the hopping gait.

The top row reveals the vanilla MB-MPO’s brittle, ”panic correction” strategy. The phase-space plot (top left) is dominated by an extreme hotspot of feedback effort (Jacobian norm  $> 2000$ ), which corresponds to a last-ditch, high-gain reaction to prevent falling when the agent is leaned far back. The time-series plot (top right) shows the dynamic signature of this strategy: a somewhat irregular hopping pattern punctuated by massive, periodic spikes in feedback effort that align perfectly with the bottom of each hop.

In stark contrast, the bottom row demonstrates the superior strategy learned by our regularized agent. The phase-space portrait (bottom left) is entirely free of the ”panic” hotspot; feedback effort is now distributed smoothly and proactively across the balancing cycle with a much lower peak magnitude ( $< 700$ ). The corresponding time-series (bottom right) shows the result: a more regular, higher, and more stable hopping gait, achieved with dramatically lower and smoother control effort. This comparison clearly visualizes the shift from a novice’s reactive, high-impact hopping to an expert’s efficient, spring-like motion, directly confirming the benefits of the minimum attention.

These evolutionary snapshots reveal that the minimum attention does more than just suppress final sensitivity values. It fundamentally alters the learning process, guiding the policy away from generic, reactive solutions and towards the discovery of specialized, structured, and efficient motor skills that distinguish expert control from novice behavior.

## OVERALL INTERPRETATION

Across all analyses, we see a consistent narrative: the minimum attention regularizer guides the agent away from brittle, reactive strategies and towards proactive, efficient, and physically intuitive motor skills. This shift directly explains the quantitative improvements in reward, energy efficiency, and stability documented in Table 2.

### 4.6 Analysis on the meta-learning functionality of minimum attention

First, for the agent of Half-Cheetah, model perturbation is realized by crippled leg and mass gain or loss. Environmental perturbation is posed by variation in floor angle emulating running uphill and downhill. The details for the agent of Hopper and Walker2D are expanded in Appendix B.

Figure 11 shows the competence of minimum attention with outperforming total rewards and reduced variances. Common observations imply non-uniform sensitivity: both policies show that their sensitivity (how much the action changes with small state changes) is not uniform across the state space slice. When we look at this specific 2D projection of the high-dimensional state space, we can see that the policy’s sensitivity changes dramatically depending on where we are in that cross-section. This is expected for non-linear policies. Regarding regions of high sensitivity, both plots have distinct regions where the sensitivity is much higher (brighter colors) than others (darker purples).

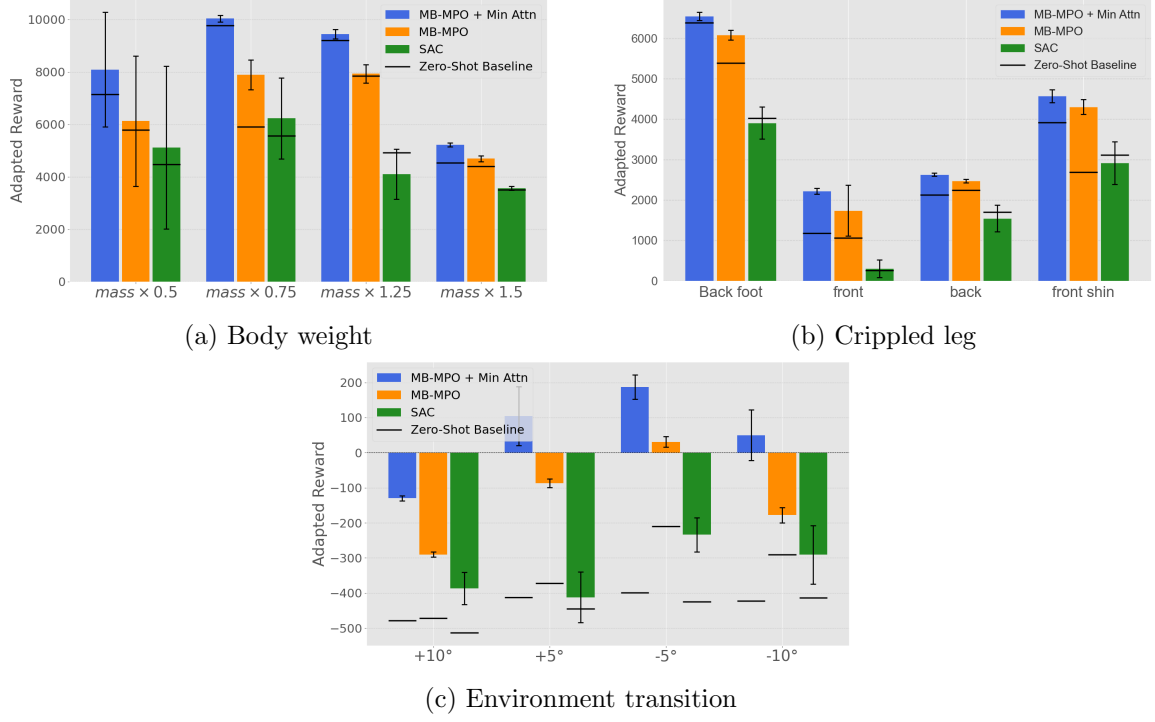


Figure 11: Half-Cheetah: Meta-testing from (a) body weight loss or gains (Easy out-of-distribution tasks), (b) crippled legs of half-cheetah (Medium out-of-distribution tasks), (c) environmental transitions to uphill and downhill (Difficult out-of-distribution tasks). This is the comparison among MB-MPO, MB-MPO + minimum attention ( $\alpha = 1.0$ ) and SAC in the adaptation from out-of-distribution Task. This is to show the adapted performance of the algorithm during testing on a completely unseen task. The experiment is run with 10 episodes. The involving variances are significantly reduced from minimum attention.

## 5 Conclusion

The formalism of minimum attention is shown to have a significant signature of dexterity to mitigate the variance in training learning curves and meta-testing. This is an important feature in designing a safe and less biased policy. Also, the regularization of minimum attention, even though with an implication of conservative minimal changes in state and time, demonstrates few sampling in out-of-distribution meta-testing and domain adaptation. The regularization of minimum attention can be further explored in its application in algorithmic debiasing and multi-task learning. It is intriguing whether singularities and rare events can be degenerate in the open avenues of language models from minimum attention. The functionality of minimum attention was explored based on the model-based RL of MB-MPO. The motor learning and control from agents of Half-Cheetah, Hopper, Walker2D, and Humanoid (Figure 3) can be further extended to other models. It needs more exploration to characterize how this formalism works in model-free RLs and to overcome the limitations of gradient-based meta-learning via multi-task learning. Also, there

needs theoretic analysis for the boundedness and stability of minimum attention based on control Lyapunov functions, where Thompson sampling can be one reference.

### Acknowledgments and Disclosure of Funding

P. Lee gives thanks to Frank C. Park introducing the formalism of minimum attention by Roger Brockett. S. Gupta and P. Lee were partially supported by NIH Data Science and NIMHD grant, 3U54MD013376-04S3. P. Lee was partially supported by Center for Equitable AI and Machine Learning Systems (CEAMLS) Affiliated Project (ID: 10072401).

### References

R. Brockett. Minimu attention control. *Proceedings of the 36th conference on Decision and Control*, 1997.

G. Brockman, V. Cheung, L. Petterson, J. Schneider, J. Schulman, J. Tang, and W. Zaremba. Openai gym. Technical report, OpenAI, 2016.

I. Clavera, J. Rothfuss, J. Schulman, Y. Fujita, T. Asfour, and P. Abbeel. Model-based reinforcement learning via meta-policy optimization. *2nd Conference on Robot Learning*, 2018.

A. Corenflos, J. Thornton, G. Deligiannidis, and A. Doucet. Differentiable particle filtering via entropy-regularized optimal transport. *ICML*, 2021.

G. Denevi, M. Pontil, and C. Ciliberto. The advantage of conditional meta-learning for biased regularization and fine tuning. *NeurIPS*, 2020.

J. Du, J. Futoma, and F. Doshi-Velez. Model-based reinforcement learning for semi-markov decision processes with neural odes. *NeurIPS*, 2020.

C. Finn, P. Abbeel, and S. Levine. Model-agnostic meta-learning for fast adaptation of deep networks. *34th ICML*, 2017.

M. Gunzburger and S. Manservisi. The velocity tracking problem for navier-stokes flows with boundary control. *SIAM J Control. Optim.*, 39:594–634, 2000.

T. Haarnoja, A. Zhou, P. Abbeel, and S. Levine. Soft actor-critic: Off-policy maximum entropy deep reinforcement learning with a stochastic actor. *Proceedings of the 35th International Conference on Machine Learning*, pages 1861–1870, 2018.

J. Hoffman, D. Roberts, and S. Yaida. Robust learning with jacobian regularization. *arXiv*, page 1908.02729, 2019.

T. Kurutach, I. Clavera, Y. Duan, A. Tamar, and P. Abbeel. Model-ensemble trust-region policy optimization. *ICLR*, 2018.

K. Lee, Y. Seo, S. Lee, H. Lee, and J. Shin. Context-aware dynamics model for generalization in model-based reinforcement learning. *ICML*, 2020.

P. Lee and F. Park. On the existence and computation of minimum attention optimal control laws. *IEEE Transactions on automatic control*, 67:2576–2581, 2022.

V. Mnih, K. Kavukcuoglu, D. Silver, A. Rusu, J. Veness, M. Bellemare, M. Graves, M. Riedmiller, A. F. G. Ostrovski, S. Petersen, C. Beattie, A. Sadik, I. Antonoglou, H. King, D. Kumaran, D. Wierstra, S. Legg, and D. Hassabis. Human-level control through deep reinforcement learning. *Nature*, 518:529–533, 2015.

A. Nagabandi, I. Clavera, S. Liu, R. Fearing, P. Abbeel, S. Levine, and C. Finn. Learning to adapt in dynamic, real-world environments through meta-reinforcement learning. *ICLR*, 2019.

J. Peters and S. Schaal. Policy gradient methods for robotics. *International Conference on Intelligent Robots and Systems*, 2006.

J. Schulman, S. Levine, P. Moritz, M. Jordan, and P. Abbeel. Trust region policy optimization. *Proceedings of the 31st International Conference on Machine Learning*, 2015.

J. Schulman, F. Wolski, P. Dhariwal, A. Radford, and O. Klimov. Proximal policy optimization algorithms. arXiv:1707.06347, 2017.

G. Uhlenbeck and L. Ornstein. On the theory of the brownian motion. *Physical Review*, 36:823–841, 1930.

X. Xu, J. Zhang, E. Ma, D. Son, O. Koyejo, and B. Li. Adversarially robust models may not transfer better: sufficient conditions for domain transferability from the view of regularization. *ICML*, 2022.

W. Zhou, Y. Li, Y. Yang, H. Wang, and T. Hospedales. Online meta-critic learning for off-policy actor-critic methods. *NeurIPS*, 2020.

## Appendix A. Technical Appendices and Supplementary Material

### 1. Setup / General Configuration

- Environments used
  - environments: "Half-Cheetah-v3", "Hopper-v3", "Walker2d-v3", "Humanoid-v2" from OpenAI Gym.
  - We normalized the env if the actions aren't already in [-1,1].
  - We have also normalized the rewards during training.
- Software and Hardware
  - All experiments are done in PyTorch and use OpenAI Gym, MuJoCo.
  - Hardware used for training is "NVIDIA A30"
- Baselines
  - Baseline algorithms "standard MB-MPO", and "SAC".
  - For the baseline we used the open-source implementation with minute changes to satisfy our requirements. We used unstable baseline repository ([link](#))

### 2. Algorithm Implementation Details (MB-MPO + Minimum Attention):

- Core MB-MPO Components
  - For inner and outer loop policy updates we have experimented with PPO, TRPO and SAC.
  - SAC is practically more suitable for the updates.
  - We have experimented with 4 different imaginary trajectory size: [16, 128, 256, 512].
- Minimum Attention Regularization Specification
  - The regularization term is  $||\partial u_\theta / \partial x||^2 + ||\partial u_\theta / \partial t||^2$
  - The regularization term is added to the reward with weight " $\alpha$ ".
  - We have experimented for " $\alpha$ " taking values [0.01, 0.05, 1.0, 5.0] and reported the results.
- Meta-Learning Setup
  - "Meta-learning" loop is that of Model-Agnostic Meta-Learning (MAML) structure (inner adaptation on models, outer update of meta-parameters).
  - Tasks (models) are sampled randomly from the task list, the mini-batch of  $R_i$  in Algorithm 1.
  - Specifications of the inner loop and outer loop is in parameter file.
- Model Ensemble Setup
  - We have experimented with four different models of ensemble size: [1, 5, 15, 20] and reported the results.

### 3. Neural Network Architectures: The following architecture is for Half-Cheetah-v3 training.

- Policy network (actor): The policy network is a multi-layer perceptron (MLP) that maps states to the parameters of a Gaussian action distribution.
  - Input layer: matches the observation dimension of the specific environment (e.g., 17 for Half-Cheetah-v3).
  - Hidden layers: two hidden layers, each with 256 units.
  - Hidden activation: ReLU is used as the activation function after each hidden layer.
  - Output layer (mean): produces the mean of the Gaussian distribution, with dimensionality matching the action space of the environment. This layer uses an identity activation. The output is subsequently passed through a tanh function and scaled/biased to the environment’s action range.
  - Output layer (log standard deviation): the log standard deviation (log std) for the Gaussian distribution is produced by a separate output head. The log std values are clamped (e.g., between -20 and 2, a common SAC practice).
  - Reparameterization trick: used (reparameterize: true) for backpropagation through the sampling process.
  - Log probability stabilization: employed (stabilize log prob: true) using the standard SAC transformation for tanh-squashed Gaussian distributions.
- Q-networks (critics): two separate Q-networks are used (typical for SAC to mitigate overestimation bias), each an MLP that maps state-action pairs to a Q-value.
  - Input layer: matches the sum of observation and action dimensions.
  - Hidden layers: two hidden layers, each with 256 units.
  - Hidden activation: ReLU.
  - Output layer: a single unit producing the Q-value, using an identity (identity) activation.
- Dynamics model ensemble: the dynamics model consists of an ensemble of ensemble size probabilistic neural networks. Each network in the ensemble predicts the change in state ( $\Delta$  state) and the reward.
  - Input layer: matches the sum of observation and action dimensions (from the previous time step).
  - Hidden layers: four hidden layers, each with 200 units.
  - Hidden activation: swish.
  - Output layer: predicts  $\Delta$  state and reward. The output dimension for  $\Delta$  state matches the observation dimension, plus one for the reward. This layer uses an identity (identity) activation. dynamics models predicts mean and log variance for  $\Delta$  state to represent uncertainty.
  - Ensemble size: 7 networks.
  - Elite models: 5 elite models are selected based on holdout loss for making predictions during rollouts.
  - Input/output normalization: dynamics models normalize inputs and de-normalize outputs.

#### 4. Hyperparameters:

Key hyperparameters for the MB-MPO implementation and the baseline are detailed below. Unless specified otherwise (e.g., for attention  $\alpha$  regularization), these values were kept constant across experiments.

- General and SAC agent parameters:
  - Optimizer (for policy, Q-networks, alpha): Adam
  - Policy network learning rate: 3e-4
  - Q-network learning rate: 3e-4
  - Discount factor ( $\gamma$ ): 0.99
  - Target smoothing coefficient ( $\gamma$ ): 0.005
  - Initial alpha (entropy coefficient): 0.2 (if not automatically tuned from the start)
  - Reward scale: 1.0
  - Entropy tuning (SAC alpha):
    - \* Automatic Tuning: Enabled (automatic tuning: true)
    - \* Target Entropy: -3 (equal to -action dim for Half-Cheetah)
    - \* Alpha Optimizer Learning Rate: 3e-4
- Dynamics model parameters:
  - Ensemble Size: 7
  - Number of Elite Models: 5
  - Optimizer: Adam
  - Learning Rate: 0.001
  - Batch Size: 256
  - Holdout Ratio (for model validation): 0.2
  - Weight Decay Coefficients:  $[2.5e-5, 5e-5, 7.5e-5, 7.5e-5, 0.0001]$  (applied to different layers).
- MB-MPO and Trainer Parameters:
  - Total Training Epochs: 400
  - Environment Steps per Epoch: 1000
  - Agent Update Batch Size: 256 (composed of real and model data)
  - Model/Environment Data Ratio for Agent Updates: 0.95 (meaning 95% model data, 5% real data per agent batch)
  - Model Training Interval: 250
  - Number of Agent Updates per Environment Step: 2
  - Rollout batch size (initial states for model rollouts): 100,000
  - Rollout mini-batch Size (for processing rollouts): 10,000
  - Warmup timesteps (random actions): 5000
  - Real Environment Replay Buffer Size: 1,000,000
  - Model-Generated Data Replay Buffer Size (per task/model if meta): 2,000,000

- Meta-Learning Parameters:
  - Number of Training Tasks: 5
  - Number of Tasks Sampled per Meta-Epoch: 5
  - Number of Tasks per Meta-Gradient Update: 5
  - In tasks are small variations in Gravity and Friction of the surface.
- Minimum attention regularization:
  - attention  $\alpha$ : Varied across experiments (e.g., 0 for vanilla, and other values like 0.01, 0.05, 0.1, etc., for adjustment in regularization). This is the main parameter we change.

## 5. Evaluation protocol and metrics:

- General evaluation:
  - We have used 10 random seeds for training runs.
  - For final evaluation of a trained agent, we run for 10 episodes run per seed.
  - Metrics reported: Average total reward, standard deviation/error of reward across seeds/episodes.
- Specific metrics (as discussed):::
  - Average Jacobian norm: during evaluation we run the trained agent for 10 evaluation episode and averaged  $\|\partial u / \partial x\|^2$  per step over 10 evaluation episodes.
  - Average action jerk: define as averaged  $\|\partial u / \partial t\|^2$  over 10 evaluation episodes.
  - Average Energy: define as “control cost”  $\text{sum}(u^2)$  per step.
- Quantification of regularization:
  - Heatmap of the Jacobian norm between the baselines to qualitative judge the impact of minimum attention regularizer.

## 6. Specific Experiments Conducted:

- Meta training:
  - To analyze the effect of attention weight, we trained agents with attention weight values  $\alpha \in \{0, 0.01, 0.05, 1.0, 5.0\}$  while keeping all other hyperparameters same.
  - To analyze the effects of the number of ensemble models, we trained 4 different sizes = [1, 5, 15, 20].
  - To analyze the effect of the imaginary trajectory size in the MB-MPO core loop, we trained 4 different agents [16, 128, 256, 512].
  - Analysis of policy sensitivity during training
- Meta testing:
  - Experiments for “out of distribution” task and fast adaptation during meta loop test time evaluation.
  - Perturbation in agent: crippled leg, mass change

- Perturbation in the environment: slope change
- For each of these experiments we note the total reward, standard deviation between runs, average Jacobian norm, average action jerk, and average energy consumed.
- Heatmap:
  - With the meta trained agent we have evaluated the impact of minimum attention regularizer on the learning process by conducting qualitative analysis by visualizing policy sensitive across different observational dimension of the environment. The goal is to pick dimension that are critical for their respective locomotion and balance challenges. Specifically we have picked
  - For Half-Cheetah
    - \* Z-coordinate versus X-velocity
    - \* X-velocity versus Z-velocity
    - \* X-velocity versus Y-angular velocity (torso)
  - For Hopper
    - \* Torso angle versus torso height
    - \* Torso angle versus torso angular velocity
    - \* Torso X-velocity versus torso angle
  - For Walker2D
    - \* Torso height versus torso angle
    - \* Torso angle versus torso angular velocity
    - \* Torso X-velocity versus torso angle
  - For Humanoid
    - \* Torso height versus torso forward velocity
    - \* Right hip angle versus left hip angle

## Appendix B. Detailed Analysis of Policy Sensitivity Heatmaps

This section provides a detailed interpretation of the policy sensitivity heatmaps for each environment, complementing the summary in the main text. In all figures, the left column corresponds to the vanilla MB-MPO baseline, and the right column corresponds to our method, MB-MPO with Minimum Attention.

### B.1 Hopper (Figure S1)

For the Hopper, the regularizer enforces a more structured and efficient balancing strategy.

- (a) **Torso angle vs. height:** The vanilla policy is highly reactive when the Hopper is leaning backward (negative Torso Angle), a critical state for falling. The regularized policy significantly dampens this peak sensitivity, suggesting it has learned a smoother, less “panicked” method for balance recovery.
- (b) **Torso angle vs. angular velocity:** In the critical balancing phase space, the regularized policy shows more focused, distinct bands of sensitivity. This is in

contrast to the broader, more diffuse sensitivity of the vanilla policy, indicating a more specialized and precise reactive control for managing angular momentum.

- (c) **Torso X-velocity vs. torso angle:** The sensitivity patterns of the regularized policy are visibly cleaner and more structured, suggesting a more coherent and principled relationship between forward speed and balancing posture compared to the patchy, reactive strategy learned by the baseline.

## B.2 Walker2D (Figure S4)

In the Walker2D environment, the regularization induces a fundamental shift in control strategy, moving from reactive fall-prevention to proactive gait management.

- (a) **Torso angle vs. height:** The most striking change is that our regularized policy almost completely eliminates the high sensitivity to backward leans that dominates the vanilla policy. Instead, it develops a new, strong diagonal band of sensitivity corresponding to states with *forward lean* and changing torso height. This suggests a strategic shift from simple fall correction to proactive control of posture during the forward phase of a stride.
- (b) **Torso angle vs. angular velocity:** The regularized policy concentrates its sensitivity in a distinct region of high forward lean and positive angular velocity. This indicates it has learned to pay specific attention to controlling its posture at the apex of a forward stride, a hallmark of a more advanced and efficient gait.
- (c) **Torso X-velocity vs. torso angle:** Again, the regularized policy’s sensitivity map is significantly more structured, reinforcing the conclusion that it has learned a smoother, more principled gait strategy that better coordinates speed and balance, rather than relying on a patchwork of reactive corrections.

## B.3 Humanoid (Figure S7)

For the highly complex Humanoid, the regularization drastically simplifies the control problem by encouraging the discovery of more efficient and specialized gait mechanics.

- (a) **Torso height vs. forward velocity:** The vanilla policy exhibits scattered, high-sensitivity “islands,” indicating a complex, reactive strategy. Our regularized policy discovers a remarkably simpler solution: its sensitivity is almost entirely focused in a narrow band at maximum torso height. This corresponds to the critical transition phase at the apex of a step, allowing the policy to be “calm” and smooth everywhere else, demonstrating a highly efficient gait.
- (b) **Hip angle coordination:** The vanilla policy shows broad sensitivity during stride transitions (when legs are in opposition). Our regularized policy dramatically focuses this sensitivity into a single, sharp hotspot. This suggests a shift from a novice, generally reactive gait to an expert one that applies precise control only at the most critical moment of weight transfer and power generation, thereby increasing efficiency and stability.

	MB-MPO	MA ( $\alpha = 1.0$ )	MA ( $\alpha = 0.01$ )	MA ( $\alpha = 0.05$ )
Early stage of epoch: 10K				
Average total rewards	$-1084 \pm 73$	<b><math>672 \pm 67</math></b>	$-427 \pm 68$	$-579 \pm 170$
Average feedback normalized	$38 \pm 3.95$	<b><math>13 \pm 0.35</math></b>	$36 \pm 5.91$	$26 \pm 1.91$
Average feedforward normalized	$7.11 \pm 0.06$	<b><math>7.33 \pm 0.04</math></b>	$5.99 \pm 0.05$	$6.86 \pm 0.06$
Average energy normalized	$363 \pm 1.68$	<b><math>320 \pm 1.55</math></b>	$327 \pm 1.51$	$350 \pm 0.96$
Middle stage of epoch: 100K		.		
Average total rewards	$5531 \pm 127$	<b><math>6564 \pm 57</math></b>	$4242 \pm 68$	$5870 \pm 117$
Average feedback normalized	$235 \pm 25.1$	<b><math>212 \pm 17.7</math></b>	$191 \pm 13.9$	$232 \pm 25.4$
Average feedforward normalized	$5.28 \pm 0.03$	<b><math>5.01 \pm 0.07</math></b>	$3.78 \pm 0.11$	$5.69 \pm 0.08$
Average energy normalized	$367 \pm 2.16$	<b><math>344 \pm 2.15</math></b>	$284 \pm 1.56$	$356 \pm 2.20$

Table S1: Half-Cheetah: Meta-training on the maturation of meta-learning

	MB-MPO	MA ( $\alpha = 1.0$ )	Ours ( $\alpha = 0.01$ )	Ours ( $\alpha = 0.05$ )
Early stage of epoch: 10K				
Average total rewards	$-1245 \pm 801$	<b><math>99 \pm 180</math></b>	$90 \pm 102$	$100 \pm 139$
Average feedback normalized	$13.6 \pm 9.23$	<b><math>21.5 \pm 1.36</math></b>	$19.2 \pm 6.8$	$15.3 \pm 1.65$
Average feedforward normalized	$10.5 \pm 0.07$	<b><math>8.12 \pm 0.15</math></b>	$5.99 \pm 0.14$	$8.07 \pm 0.08$
Average energy normalized	$425 \pm 5.68$	<b><math>330 \pm 4.54</math></b>	$320 \pm 2.05$	$350 \pm 3.15$
Middle stage of epoch: 100K				
Average total rewards	$4907 \pm 69$	<b><math>4953 \pm 85</math></b>	$4920 \pm 50$	$4950 \pm 138$
Average feedback normalized	$164 \pm 11.5$	<b><math>301 \pm 12.7</math></b>	$222 \pm 10.5$	$185 \pm 10.1$
Average feedforward normalized	$6.15 \pm 0.03$	<b><math>5.45 \pm 0.05</math></b>	$3.68 \pm 0.03$	$6.1 \pm 0.04$
Average energy normalized	$325 \pm 1.54$	<b><math>302 \pm 1.42</math></b>	$230 \pm 1.72$	$340 \pm 2.9$

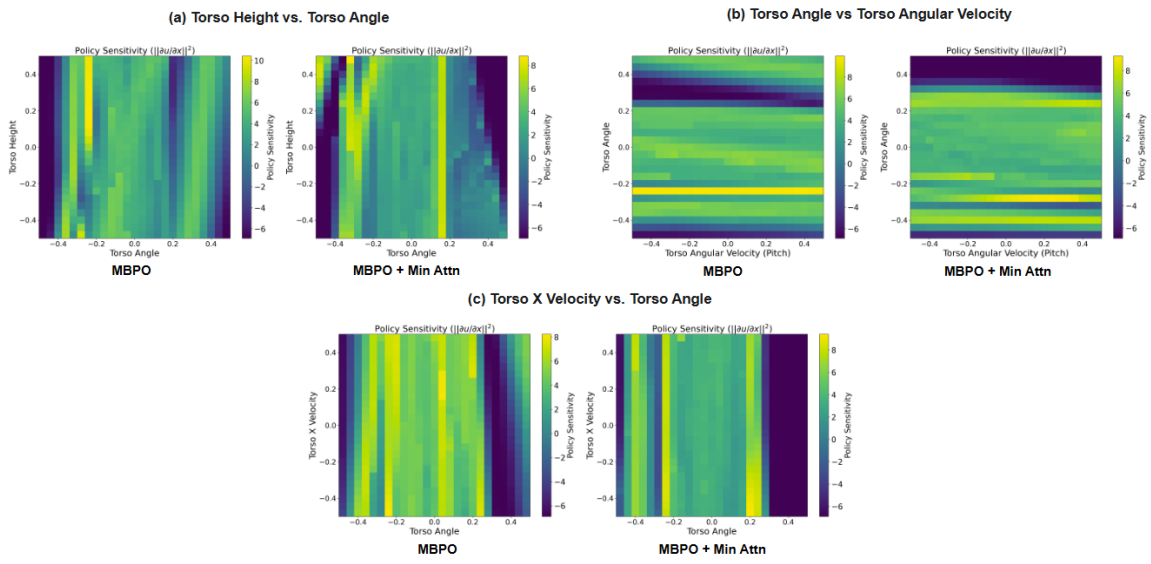
Table S2: Half-Cheetah: Meta-testing on the maturation of meta-learning

	MB-MPO	Ours ( $\alpha = 1.0$ )
Early stage of epoch: 10K		
Average total rewards	$47 \pm 2$	<b><math>232 \pm 5.75</math></b>
Average feedback normalized	$168 \pm 5.26$	<b><math>290 \pm 1.82</math></b>
Average feedforward normalized	$0.45 \pm 0.026$	<b><math>0.11 \pm 0.003</math></b>
Average energy normalized	$25.9 \pm 0.27$	<b><math>55 \pm 2.23</math></b>
Middle stage of epoch: 100K		
Average total rewards	$222 \pm 0.68$	<b><math>688 \pm 1.92</math></b>
Average feedback normalized	$42.6 \pm 3.47$	<b><math>55.1 \pm 0.68</math></b>
Average feedforward normalized	$0.007 \pm 0.003$	<b><math>0.04 \pm 0.002</math></b>
Average energy normalized	$55.4 \pm 0.388$	<b><math>219 \pm 1.66</math></b>
Final stage of epoch: 200K		
Average total rewards	$2475 \pm 3.81$	<b><math>2825 \pm 1.25</math></b>
Average feedback normalized	$507 \pm 2.23$	<b><math>153 \pm 0.73</math></b>
Average feedforward normalized	$0.05 \pm 0.008$	<b><math>0.04 \pm 0.002</math></b>
Average energy normalized	$573 \pm 2.28$	<b><math>330 \pm 0.93</math></b>

Table S3: Hopper: Meta-training

	MB-MPO	Ours ( $\alpha = 1.0$ )
Early stage of epoch: 10K		
Average total rewards	$234 \pm 3.39$	<b><math>278 \pm 3.15</math></b>
Average feedback normalized	$99.7 \pm 2.15$	<b><math>137 \pm 5.25</math></b>
Average feedforward normalized	$0.11 \pm 0.003$	<b><math>0.03 \pm 0.001</math></b>
Average energy normalized	$152 \pm 5.75$	<b><math>114 \pm 1.54</math></b>
Middle stage of epoch: 100K		
Average total rewards	$323 \pm 7$	<b><math>394 \pm 6.85</math></b>
Average feedback normalized	$49 \pm 3.67$	<b><math>89 \pm 1.26</math></b>
Average feedforward normalized	$0.11 \pm 0.004$	<b><math>0.02 \pm 0.003</math></b>
Average energy normalized	$148 \pm 5.11$	<b><math>122 \pm 10.11</math></b>
Final stage of epoch: 200K		
Average total rewards	$467 \pm 100$	<b><math>485 \pm 61</math></b>
Average feedback normalized	$162 \pm 27$	<b><math>140 \pm 10.6</math></b>
Average feedforward normalized	$0.04 \pm 0.01$	<b><math>0.02 \pm 0.002</math></b>
Average energy normalized	$258 \pm 38$	<b><math>77 \pm 1.1</math></b>

Table S4: Hopper: Meta-testing

Figure S1: Hopper: Heatmap of feedback. The feedback ( $||\partial u / \partial x||^2$ ) in the projection of the states to (a) Torso-angle versus Torso-height, (b) Torso-angle versus Torso X-velocity, and (c) Torso-angular velocity versus Torso-angle.

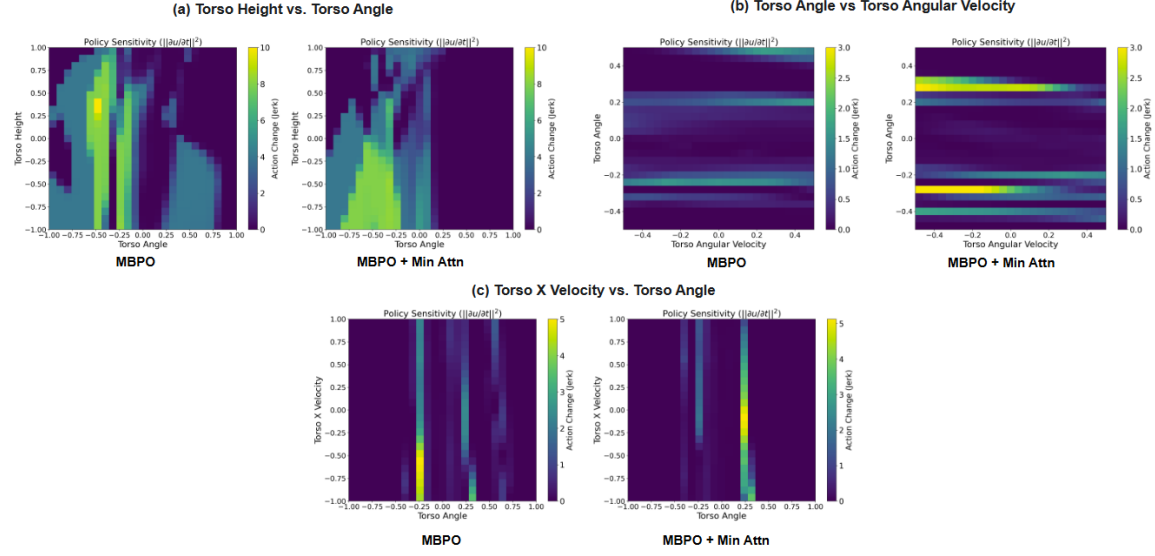


Figure S2: Hopper: Heatmap of feedforward. The feedforward ( $\|\partial u / \partial t\|^2$ ) in the projection of the states to (a) Torso-angle versus Torso-height, (b) Torso-angle versus Torso X-velocity, and (c) Torso-angular velocity versus Torso-angle.

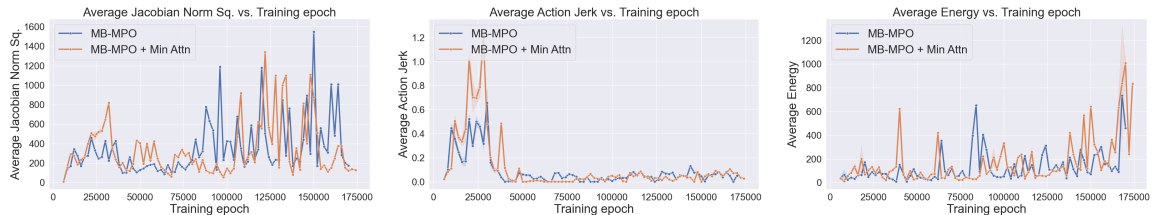


Figure S3: Hopper: Time profiles for the feedback, feedforward, and energy in meta-training. The comparison of feedback ( $\|\partial u / \partial x\|^2$ , Jacobian), feedforward ( $\|\partial u / \partial t\|^2$ , Jerk), and energy ( $\|u\|^2$ ) between MB-MPO and MB-MPO with minimum attention ( $\alpha = 1.0$ ).

	MB-MPO	Ours ( $\alpha = 1.0$ )
Early stage of epoch: 10K		
Average total rewards	$325 \pm 226$	<b><math>615 \pm 45.76</math></b>
Average feedback normalized	$3 \pm 0.33$	<b><math>60.6 \pm 1.74</math></b>
Average feedforward normalized	$7.76 \pm 0.84$	<b><math>0.35 \pm 0.07</math></b>
Average energy normalized	$969 \pm 248$	<b><math>798 \pm 84</math></b>
Middle stage of epoch: 100K		
Average total rewards	$424 \pm 108$	<b><math>1453 \pm 96</math></b>
Average feedback normalized	$88 \pm 10.4$	<b><math>49.9 \pm 2.34</math></b>
Average feedforward normalized	$0.15 \pm 0.04$	<b><math>0.09 \pm 0.02</math></b>
Average energy normalized	$412 \pm 250$	<b><math>992 \pm 295</math></b>
Final stage of epoch: 200K		
Average total rewards	$2399 \pm 694$	<b><math>3038 \pm 148</math></b>
Average feedback normalized	$129 \pm 5.25$	<b><math>210 \pm 10</math></b>
Average feedforward normalized	$0.36 \pm 0.08$	<b><math>0.37 \pm 0.06</math></b>
Average energy normalized	$2250 \pm 628$	<b><math>1860 \pm 52.2</math></b>

Table S5: Walker2D: Meta-training

	MB-MPO	Ours ( $\alpha = 1.0$ )
Early stage of epoch: 10K		
Average total rewards	$51 \pm 29$	<b><math>45 \pm 7.91</math></b>
Average feedback normalized	$4.62 \pm 0.21$	<b><math>13.1 \pm 0.7</math></b>
Average feedforward normalized	$6.47 \pm 0.25$	<b><math>3.05 \pm 0.19</math></b>
Average energy normalized	$500 \pm 42$	<b><math>394 \pm 29</math></b>
Middle stage of epoch: 100K		
Average total rewards	$662 \pm 194$	<b><math>729 \pm 132</math></b>
Average feedback normalized	$110 \pm 7.1$	<b><math>77.8 \pm 33.2</math></b>
Average feedforward normalized	$0.78 \pm 0.25$	<b><math>0.25 \pm 0.02</math></b>
Average energy normalized	$436 \pm 214$	<b><math>487 \pm 141</math></b>
Final stage of epoch: 200K		
Average total rewards	$523 \pm 174$	<b><math>1123 \pm 152</math></b>
Average feedback normalized	$150 \pm 29$	<b><math>197 \pm 10.6</math></b>
Average feedforward normalized	$0.01 \pm 0.06$	<b><math>0.07 \pm 0.07</math></b>
Average energy normalized	$624 \pm 106$	<b><math>1230 \pm 323</math></b>

Table S6: Meta-testing of Walker2D

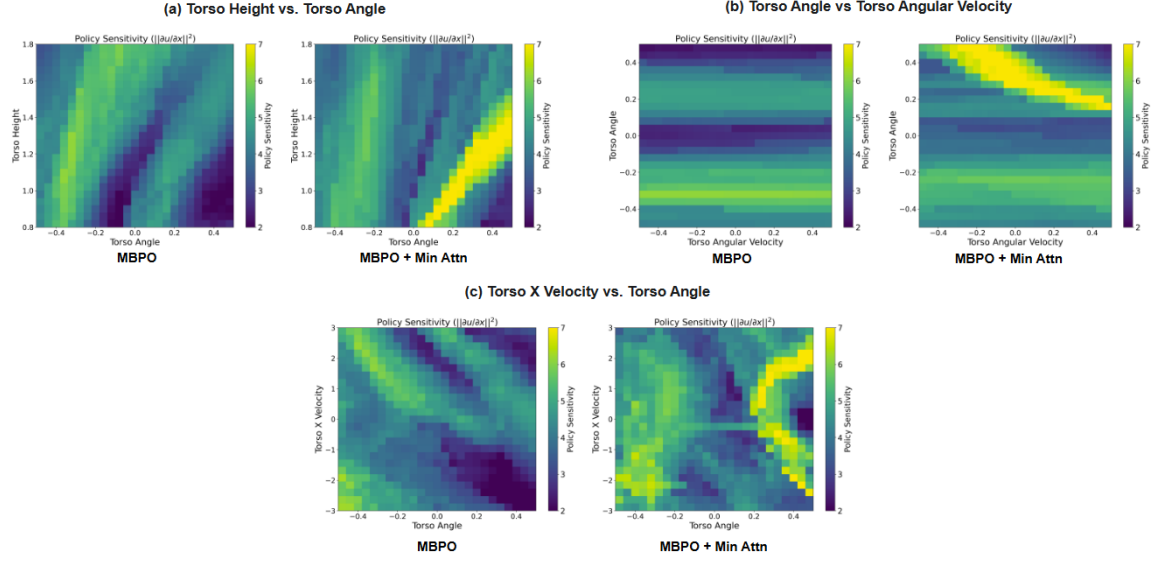


Figure S4: Walker2D: Heatmap of feedback. The feedback ( $||\partial u / \partial x||^2$ ) in the projection of the states to (a) Torse-angle versus Torse-height, (b) Torso-angle versus Torse X-velocity, and (c) Torso-angular velocity versus Torso-angle.

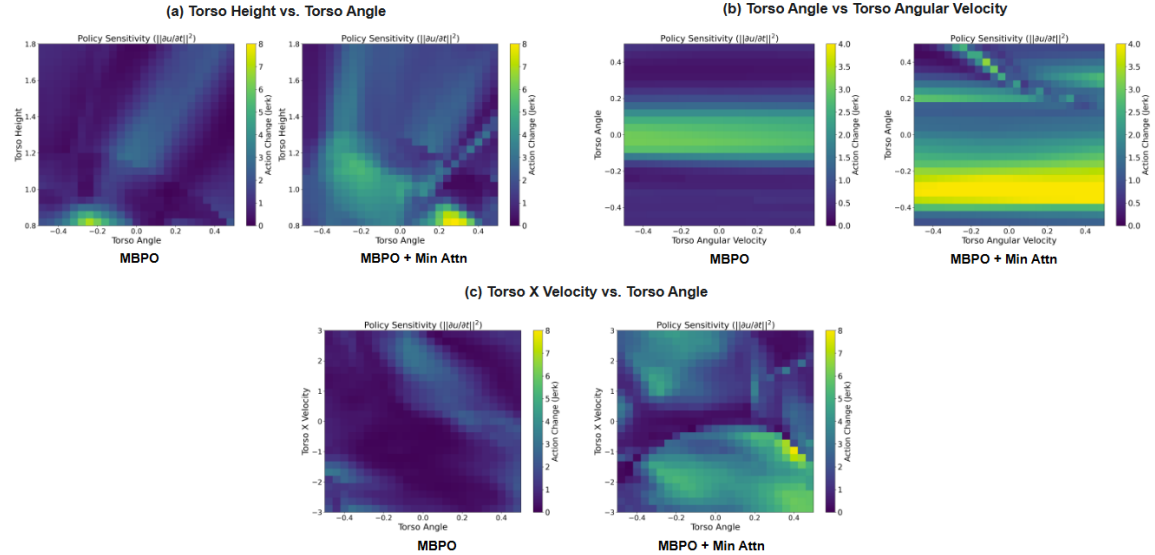


Figure S5: Walker2D: Heatmap of feedforward. The feedforward ( $||\partial u / \partial t||^2$ ) in the projection of the states to (a) Torse-angle versus Torse-height, (b) Torso-angle versus Torse X-velocity, and (c) Torso-angular velocity versus Torso-angle.

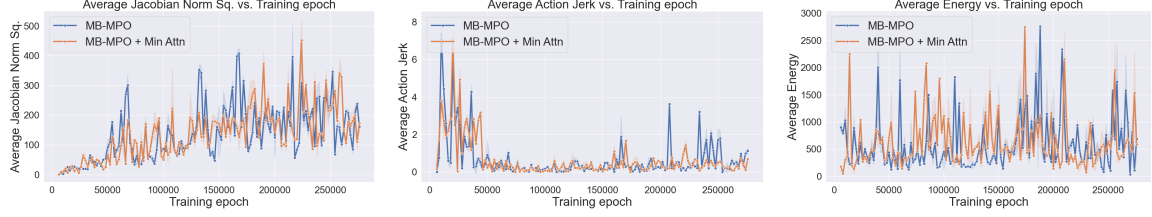


Figure S6: Walker2D: Time profiles for the feedback, feedforward, and energy in meta-training. The comparison of feedback ( $\|\partial u/\partial x\|^2$ , Jacobian), feedforward ( $\|\partial u/\partial t\|^2$ , Jerk), and energy ( $\|u\|^2$ ) between MB-MPO and MB-MPO with minimum attention ( $\alpha = 1.0$ ).

	MB-MPO	Ours ( $\alpha = 1.0$ )
Early stage of epoch: 10K		
Average total rewards	$297 \pm 10$	<b><math>245 \pm 10</math></b>
Average feedback normalized	$39.9 \pm 1.7$	<b><math>2.48 \pm 0.13</math></b>
Average feedforward normalized	$0.13 \pm 0.006$	<b><math>0.877 \pm 0.06</math></b>
Average energy normalized	$108 \pm 3.58$	<b><math>52.1 \pm 1.6</math></b>
Middle stage of epoch: 100K		
Average total rewards	$332 \pm 26$	<b><math>267 \pm 82</math></b>
Average feedback normalized	$119.2 \pm 3.82$	<b><math>57.5 \pm 10.8</math></b>
Average feedforward normalized	$0.09 \pm 0.01$	<b><math>0.42 \pm 0.07</math></b>
Average energy normalized	$64.3 \pm 4.99$	<b><math>107 \pm 8.89</math></b>
Final stage of epoch: 200K		
Average total rewards	$575 \pm 177$	<b><math>352 \pm 38</math></b>
Average feedback normalized	$187 \pm 16$	<b><math>79.1 \pm 5.49</math></b>
Average feedforward normalized	$0.516 \pm 0.05$	<b><math>0.198 \pm 0.01</math></b>
Average energy normalized	$144 \pm 42.4$	<b><math>136 \pm 8.95</math></b>

Table S7: Humanoid: Meta-training

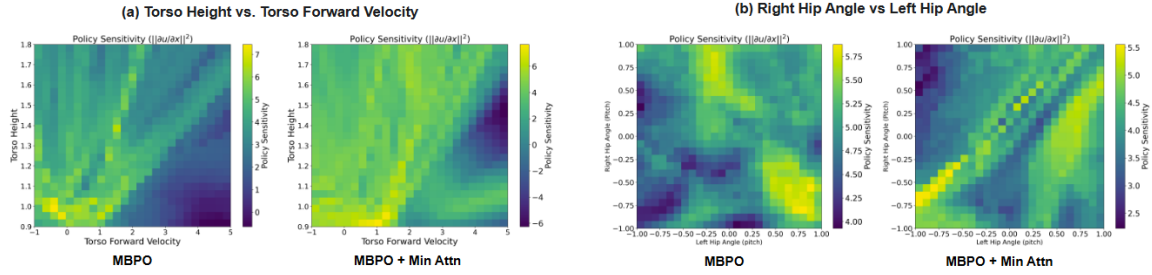
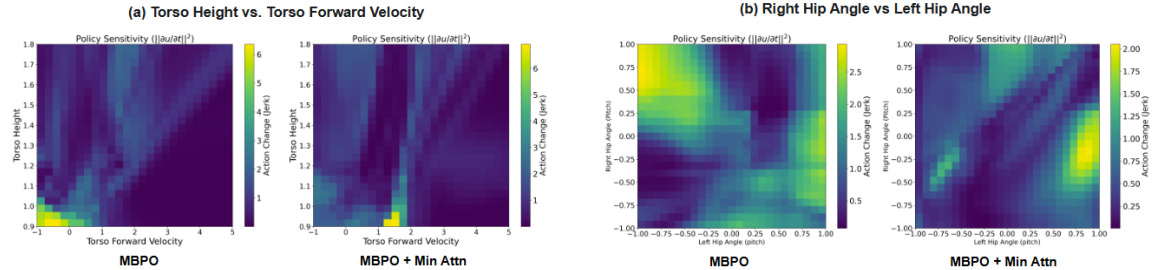
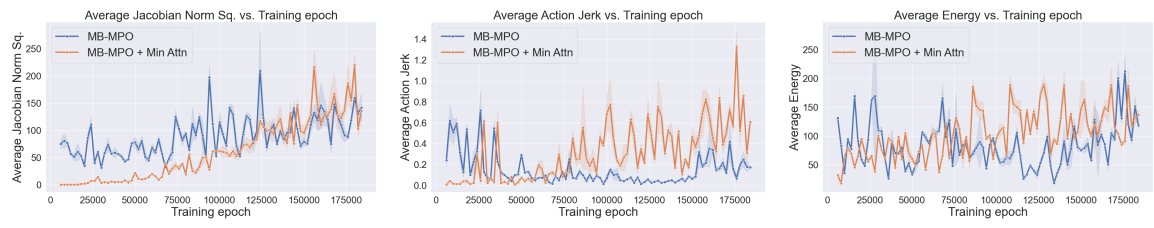


Figure S7: Humanoid: Heatmap of feedback. The feedback ( $\|\partial u/\partial x\|^2$ ) in the projection of the states to (a) Torso-height versus Torso-forward-velocity, and (b) Right-hip angle versus left-hip angle.

	MB-MPO	Ours ( $\alpha = 1.0$ )
Early stage of epoch: 10K		
Average total rewards	$314 \pm 19$	<b><math>359 \pm 27</math></b>
Average feedback normalized	$59.1 \pm 5.24$	<b><math>15.9 \pm 1.06</math></b>
Average feedforward normalized	$0.285 \pm 0.003$	<b><math>0.136 \pm 0.002</math></b>
Average energy normalized	$101 \pm 8.21$	<b><math>53.3 \pm 0.811</math></b>
Middle stage of epoch: 100K		
Average total rewards	$351 \pm 91$	<b><math>395 \pm 27</math></b>
Average feedback normalized	$76.3 \pm 13.6$	<b><math>36 \pm 4.32</math></b>
Average feedforward normalized	$0.13 \pm 0.03$	<b><math>0.16 \pm 0.09</math></b>
Average energy normalized	$73.1 \pm 21.9$	<b><math>140 \pm 9.42</math></b>
Final stage of epoch: 200K		
Average total rewards	$315 \pm 67$	<b><math>480 \pm 34</math></b>
Average feedback normalized	$277 \pm 64.1$	<b><math>76.3 \pm 11.7</math></b>
Average feedforward normalized	$0.332 \pm 0.11$	<b><math>0.09 \pm 0.01</math></b>
Average energy normalized	$11 \pm 16$	<b><math>188 \pm 20.8</math></b>

Table S8: Meta-testing of Humanoid

Figure S8: Humanoid: Heatmap of feedforward. The feedforward ( $\|\partial u / \partial t\|^2$ ) in the projection of the states to a) Torso-height versus Torso-forward-velocity, and b) Right-hip angle versus left-hip angle.Figure S9: Humanoid: Time profiles for the feedback, feedforward, and energy in meta-training. The comparison of feedback ( $\|\partial u / \partial x\|^2$ , Jacobian), feedforward ( $\|\partial u / \partial t\|^2$ , jerk), and energy ( $\|u\|^2$ ) between MB-MPO and MB-MPO with minimum attention ( $\alpha = 1.0$ ).